18th International Conference on Information Fusion
Washington, DC - July 6-9, 2015

Information Fusion with Belief Functions: a comparison of Proportional Conflict Redistribution PCR5 and PCR6 rules for Networked Sensors

Roman Ilin
Sensors Directorate
Air Force Research Laboratory
Wright Patterson AFB, OH, USA
rilin325@gmail.com

Erik Blasch
Information Directorate
Air Force Research Laboratory
Rome, NY, USA
erik.blasch@gmail.com

***Abstract*—We compare several belief fusion methods, including the proportional conflict redistribution rules (PCR5 and PCR6) for multiple sources. The PCR fusion of evidence methods have shown improvement over the classical Dempster-Shafer and Bayesian fusion techniques in the presence of conflicting information. The PCR6 rule shows improvement over PCR5 when the number of sources increases. Using Hasse graphical diagrams, we highlight the comparison between the methods. To our knowledge, this is the first such comparison between PCR5 and PCR6 with more than two sources. The results point toward a transition between PCR5 and PCR6 at three sources.**

Keywords—Probability, Belief Functions, Conflicting Data, Sensor Networks, Hasse Diagram

I. INTRODUCTION

Over the past decade, there have been numerous discussions on the proportional conflict redistribution rules (PCR) in evidential belief functions. A comprehensive analysis of belief functions includes Bayesian methods, Dempster-Shafer theory (DST), and Dezert-Smarandache theory (DSmT), as the origin of the PCR rules [1]. The most current PCR5 and PCR6 rules address the limitation of the DS rule for combining potentially highly conflicting sources of evidence by redistributing the belief mass. In the literature, few investigations directly compare the performance of PCR5 versus PCR6 and if so, only for small number of sources.

Hongfei *et al*. [2] compared PCR1-PCR6 with two sensors for three class classifications and found equivalent performance while suggesting PCR6f with a distribution proportion variation based on the global basic belief assignment (gbba). In another study by Smarandache and Dezert [3], PCR5 and PCR6 are compared for two priors and three classes with additions of a PCR5 fusion-conditional rule.

The origins of the PCR rules development begin with the classic paper in 2005 [4] for two sources. In 2006, a summary of DSmT was provided in [5] and Martin and Osswald presented PCR6 [6] for multiple sources. Together, in 2008, these groups combined for a summary of qualitative and quantitative belief combination rules [7].

The belief analysis using PCR has been applied to many areas showing promise for different applications [8], [9], [10]. One area of interest is target tracking which began with DS methods [11], [12], [13]. Tracking, classification, and identification included the Joint-Belief Probability Data Association Filter (JBPDAF) with imagery intelligence (IMINT) with a DST classification. A update to DST included PCR5 tracking by Dezert and Tchamova *et al*. [14] and Dambreville *et al*. using the PCR6 [15]. Pannetier *et al*. combined the PCR methods for tracking and classification with IMINT [16] along with interactive multiple model (IMM) approaches [17]. Other cases include the particle filter (PF) with the PCR5 [18]. Finally, a recent update included the Tchamova, J. Dezert T-Conorm-Norm (TCN) as comparisons with the PCR5 fusion rule, Dempster's rule, and updates with the fuzzy fusion rules [19].

The relationships between DST, DSmT, and Bayesian approaches are demonstrated in Figure 1, which is based on J. Dezert's DSmT tutorial. Each source assigns conditional probabilities to possible target classes, given observed measurements. In the Bayesian approach, the probabilities are fused directly. DST and DSmT introduce additional levels of uncertainty representation and methods for conflict redistribution.

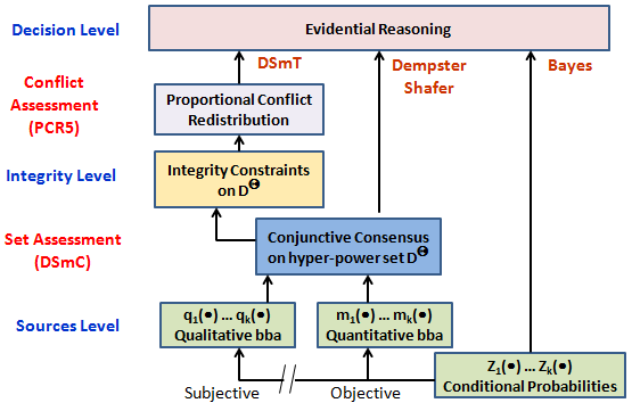

Figure 1 Comparison of Bayesian, Dempster-Shafer, and PCR5 Fusion Theories

Along with the comparisons and applications of the PCR5 and PCR6 (although individually), there were developments in the PCR assessments. In particular, the relationship between DST

and Bayesian methods was investigated in [20] with the following conclusion:

> *"Only in the very particular case where the basic belief assignments to combine are Bayesian and when the prior information is uniform (or vacuous), the Dempster's rule remains consistent with the Bayes fusion rule., Dempster's rule is incompatible with the Bayes rule and it is not a generalization of the Bayes fusion rule"*

Recently, the PCR6 was compared to an averaging rule [21]. A sensitivity comparison was then made [22] over the many rules including Dempster's rule, Yager's rule, Florea's robust combination rule (RCR), disjunctive rule, Dubois and Prade's rule, proportional conflict redistribution rule (PCR5), and mean rule [8]; however PCR6 was not included in the comparison.

The review here presents an interesting development. In most cases, either the PCR5 or the PCR6 were used and typically compared to DST methods. In no cases, were they compared together for tracking and classification. Work by Blasch *et al*. [1] aimed to compare DST, Bayes, and PCR. The comparison demonstrated the benefits of PCR over DST and Bayes, but the study was limited as the PCR5 and PCR6 rules are the same for two source fusion.

In this study, we seek to compare PCR5 with PCR6 with three and more sources, and thus add to the discussion of PCR rules. The rest of the paper is as follows. Sect. II discusses belief formalisms. Sect III introduces PCR5 and Sect. IV PCR6. Sect. V does a comparison. Finally, Sect. VI and VII provide discussion and conclusions. In addition to the performance comparison, we utilized graphical illustrations of PCR5 and PCR6 rules with Hasse diagrams in order to clarify the differences between the two.

II. BELIEF FUNCTIONS FORMALISM

Dempster-Shafer theory assumes a finite set Ω of possible answers to a question, referred to as the *frame of discernment.* The events correspond to subsets of Ω, with their uncertainty quantified by the *basic probability assignment, or bpa* (also referred to as *basic belief assignment, or bba*), which is a function $m: 2^{\Omega} \rightarrow [0,1]$ such that

$$m(\emptyset) = 0, \tag{1}$$

and

$$\sum_{A \subseteq \Omega} m(A) = 1. \tag{2}$$

The key idea here is that not all subsets of Ω encode inferred information; some are basic events and can be assigned basic (elementary) probability mass. Those subsets that we assign non-zero $m()$ are called *focal elements*. This structure is called a *body of evidence*. In the most general case all subsets of Ω (all elements of the powerset of Ω) may serve as focal elements, however in practice the set of focal elements is a subset of the powerset.

DSmT generalizes the frame of discernment Ω to consist of possibly overlapping sets. Overlapping sets highlights that the full set of possible events includes all possible intersections and unions of the elements of Ω -which is a larger set of events than that of DST. In this work we only consider the Dempster model.

A belief function $Bel: 2^{\Omega} \rightarrow [0,1]$ is computed from the *bpa* as follows:

$$Bel(A) = \sum_{B \subseteq A} m(B), \tag{3}$$

where $A \subseteq \Omega$. The *bpa* can be recovered from the belief function using the following formula,

$$m(A) = \sum_{B \subseteq A} (-1)^{|A \setminus B|} Bel(B). \tag{4}$$

Thus there is a one-to-one correspondence between m and Bel. The belief functions satisfy the following properties:

$$Bel(\emptyset) = 0, \qquad Bel(\Omega) = 1,$$

$$Bel\left(\bigcup_{i=1}^{n} A_i\right) \geq \sum_{I \subset \{1,2..n\}, I \neq \emptyset} (-1)^{|I|+1} Bel\left(\bigcap_{i \in I} A_i\right). \tag{5}$$

The last property shows that belief functions are non-additive [8] even in the case of two disjoined subsets A and B: $Bel(A \cup B) \geq Bel(A) + Bel(B)$, in contrast to additivity of probability functions. If, and only if, the focal elements of *bpa* are 1-element subsets ("singletons") of Ω, does Bel become equivalent and reduces to a probability function.

A combination of evidence coming from different sources is a key feature of DST. Given two bodies of evidence with *bpa*'s $m_1$and m_2 that are combined or "fused", the *conjunctive rule* is given by the following formula:

$$m_{1 \cap 2}(A) = \sum_{B \cap C = A} m_1(B) m_2(C). \tag{6}$$

The result of (6) needs to be normalized in order to satisfy (2). Dividing $m_{1 \cap 2}$ by *1-K* achieves normalization, with

$$K = \sum_{B \cap C = \emptyset} m_1(B) m_2(C). \tag{7}$$

Formulas (6) and (7) correspond to the Dempster's rule of combination. The un-normalized version (6) of the Dempster's rule is used in Transferable Belief Models [23].

The quantity *K*is referred to as the *total conflicting mass*. The classical Dempster's rule is inconsistent in the presence of conflicting evidence, as has been shown recently in [20], although the inconsistencies have been pointed out by earlier researchers, starting with Lotfi Zadeh. Therefore, other combination rules have been proposed. We consider the Proportional Conflict Redistribution rules (PCR5 and PCR6

rules) proposed in [4], [6]. The main idea behind the PCR rules is to consider each term in the total conflicting mass separately and redistribute the mass of the term to the events involved in this term's conflict. The next sections provide a detailed description of these rules.

III. Proportional Conflict Redistribution 5 (PCR5)

The general formulas for PCR5 and PCR6 are given in [4], and [6] respectively. Due to large number of indices and nested summations, they are difficult to understand. Several examples of these formulas for simple cases are given in the earlier publications, for example [5]. Here, we attempt to make the rules more understandable by illustrating them with diagrams.

We consider the fusion of an arbitrary number of sources, $S \in \{1,2,\dots\}$. The first step in both PCR5 and PCR6 is to compute the conjunctive combination of all sources, which is the generalization of (6), for all subsets of Ω, $A \subseteq \Omega$:

$$m_{\cap}(A) = \sum_{X_1 \cap X_2 \cap \dots \cap X_S = A} m_1(X_1) m_2(X_2) \dots m_S(X_S). \quad (8)$$

The total conflicting mass is given as follows,

$$K = \sum_{X_1 \cap X_2 \cap \dots \cap X_S = \emptyset} m_1(X_1) m_2(X_2) \dots m_S(X_S). \quad (9)$$

Each term in (9) is referred to as a partial conflicting mass, and is denoted by $m(X_1 \cap X_2 \cap \dots \cap X_S)$. Each partial conflicting mass is redistributed to its subsets in proportion to the basic probability mass already assigned to these subsets.

In order to illustrate the rules, we will utilize a graphical representation of a collection of sets, called Hasse diagrams. In general, Hasse diagrams represent partially ordered sets, or *posets* [24]. Poset is a set with relation of partial order defined on it. This relation is usually referred to as "less than", denoted by $\leq$. On the diagrams, the elements of a poset are shown as circles and the related elements are connected by lines. In the case of sets, two sets are related if one of them is a subset of the other - in other words the relation of partial order is the set inclusion relation.

EXAMPLE 1:
Consider the case of S=3 sources. The frame of discernment contains only 2 elements, A and B, $\Omega = \{A, B\}$, with the basic probability mass assignments for each source given in Table 1. There are, of course, 4 elements in the powerset of Ω.

TABLE 1

	$\emptyset$	$\{A\}$	$\{B\}$	$\{A, B\}$
m_1		0.6		0.4
m_2			0.3	0.7
m_3			0.1	0.9

The conflicting mass is obtained by listing all set combinations from the 3 sources that result in empty intersection and have non-zero mass assignments. In this case, there are 4^3=64 combinations of sets (4 from each of the 3 sources). Out of these, we have only the following 3 partial conflicts (Table 2):

TABLE 2

Partial Conflict Terms	Values
$m_1(\{A\})m_2(\{B\})m_3(\{B\})$	0.018
$m_1(\{A\})m_2(\{A,B\})m_3(\{B\})$	0.042
$m_1(\{A\})m_2(\{B\})m_3(\{A,B\})$	0.162
Total Conflicting Mass:	0.222

Consider the first partial conflict. The redistribution of the mass (0.018) using PCR5 rule is illustrated in Fig. 2.

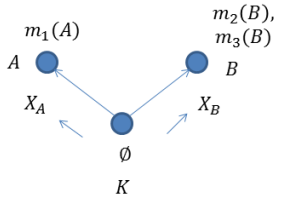

Figure 2 Redistribution of the first partial conflicting mass from Table 2 according to PCR5. X_A and X_B are the masses added to the sets A and B respectively.

The masses X_A and X_B are computed using the following formulas, with curvy brackets removed for clarity:

$$\begin{aligned} K &= m_1(A)m_2(B)m_3(B) \\ X_A &= \frac{m_1(A)}{m_1(A) + m_2(B)m_3(B)} K \\ X_B &= \frac{m_2(B)m_3(B)}{m_1(A) + m_2(B)m_3(B)} K \end{aligned} \quad (10)$$

The key feature of PCR5 is that the mass assignments coming from several sources and assigned to the same subset (B in this example) are multiplied, and after this multiplication the conflicting mass is divided proportionally to the mass in each unique conflicting subset. Thus in this example we divide K into two parts proportional to $m_1(A)$ and $m_2(B)m_3(B)$.

Consider the next partial conflict (row 2 in Table 2). The redistribution of the mass (0.042) using PCR5 rule is illustrated in Fig. 3.

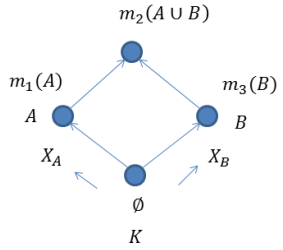

Figure 3 Redistribution of the second partial conflicting mass from Table 2 according to PCR5. X_A and X_B are the masses added to the sets A and B respectively.

Here, the masses X_A and X_B are computed using the following formulas (again with curvy brackets removed for clarity):

$$K = m_1(A)m_2(A,B)m_3(B)$$
$$X_A = \frac{m_1(A)}{m_1(A)+m_3(B)}K$$
$$X_B = \frac{m_3(B)}{m_1(A)+m_3(B)}K \quad (11)$$

In order to understand this redistribution, we invoke the concept of canonical form of the set (see [8], Vol. 2, page 209). In this case, $c(A \cap (A \cup B) \cap B) = A \cap B$, which clarifies that only the sets A and B remaining in the canonical form are in conflict with each other. The proportions of the conflicting mass K are computed with respect to the canonical form, which is why $m_2(A,B)$ is not used in the proportions. Mass $m_2(A,B)$ is used however, in the computation of K itself. The third partial conflict is resolved analogously, as shown in Fig. 4 and the formulas below.

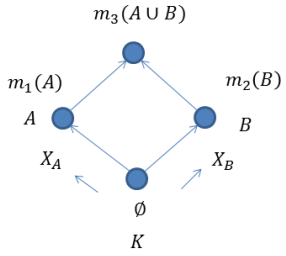

Figure 4 Redistribution of the third partial conflicting mass from Table 2 according to PCR5. X_A and X_B are the masses added to the sets A and B respectively.

The redistributed massed are given as follows.

$$K = m_1(A)m_2(A,B)m_3(B)$$
$$X_A = \frac{m_1(A)}{m_1(A)+m_3(B)}K$$
$$X_B = \frac{m_3(B)}{m_1(A)+m_3(B)}K \quad (12)$$

At this point we observe that the first partial conflict was also redistributed according to the canonical form, except we had to remember to multiply the masses assigned to the same sets by different sources. The general procedure for PCR5 appears to be as follows:

The PCR5 Procedure
1. Compute conjunctive consensus (8), (9) 2. List all partial conflicts 3. For each partial conflict, a. compute canonical form and the corresponding masses (multiplying some of them) b. Redistribute the conflict with respect to the sets in the canonical form

EXAMPLE 2:
Consider another example that illustrates the PCR5 procedure. The set Ω consists of 3 elements, $\Omega = \{A, B, C\}$. The following bodies of evidence are given in Table 3. There are now 8 elements in the powerset of Ω.

TABLE 3

	$\emptyset$	$\{A\}$	$\{B\}$	$\{A,B\}$	$\{C\}$	$\{A,C\}$	$\{B,C\}$	$\{A,B,C\}$
m_1		0.2						0.8
m_2			0.3					0.7
m_3							0.3	0.7

The following table lists the partial conflicts for this example.

TABLE 4

Partial Conflict Terms	**Values**
$m_1(\{A\})m_2(\{B\})m_3(\{B,C\})$	0.018
$m_1(\{A\})m_2(\{A,B,C\})m_3(\{B,C\})$	0.042
$m_1(\{A\})m_2(\{B\})m_3(\{A,B,C\})$	0.042
Total Conflicting Mass:	0.102

Consider the first conflict. The diagram depicting the sets involved in the conflict is given in Fig. 5.

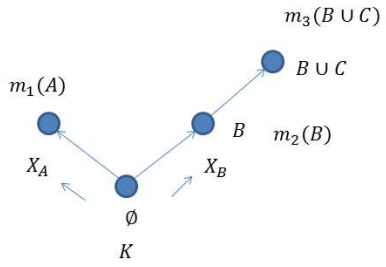

Figure 5 Redistribution of the first partial conflicting mass from Table 4 according to PCR5. X_A and X_B are the masses added to the sets A and B respectively.

In this case, the canonical form of the sets involved in the partial conflict is $c(A \cap B \cap (B \cup C)) = A \cap B$. The set $B \cup C$ disappears from the canonical form. Since $B \cup C$ was "absorbed" by B, and the two sets are not identical, and we do not multiply their weights. Thus the redistribution is done as follows:

$$K = m_1(A)m_2(B)m_3(B,C)$$
$$X_A = \frac{m_1(A)}{m_1(A)+m_2(B)}K$$
$$X_B = \frac{m_2(B)}{m_1(A)+m_2(B)}K \quad (13)$$

In the second conflict, we obtain the following diagram:

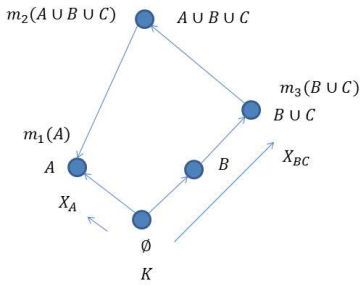

Figure 6 Redistribution of the second partial conflicting mass from Table 4 according to PCR5. X_A and X_{BC} are the masses added to the sets A and BC respectively.

The canonical form for this conflict is $c(A \cap (B \cup C) \cap (A \cup B \cup C)) = A \cap (B \cup C)$. There are no masses that need to be multiplied. Thus, the redistribution is computed as follows:

$$\begin{aligned} K &= m_1(A)m_2(A,B,C)m_3(B,C) \\ X_A &= \frac{m_1(A)}{m_1(A)+m_3(B,C)}K \\ X_{BC} &= \frac{m_2(B,C)}{m_1(A)+m_3(B,C)}K \end{aligned} \quad (14)$$

Next we discuss PCR6 in a similar graphical manner.

IV. Proportional Conflict Redistribution 6 (PCR6)

The PCR6 rule was proposed as simplification of PCR5 [6]. The general formula for PCR6 is also complex and can be difficult to understand. Here we present PCR6 as a procedure illustrated with diagrams and tables. The procedure for PCR6 can be summarized as follows.

The PCR6 Procedure
1. Compute conjunctive consensus (8), (9)
2. List all partial conflicts
3. For each partial conflict, redistribute the conflict to the sets involved in the conflict proportionally relative to their masses.

The transformation to canonical form is absent here and also the multiplication of the mass assigned to the same sets by different sources.

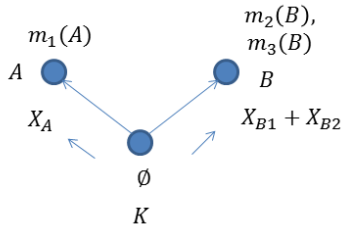

Figure 7 Redistribution of the first partial conflicting mass from Table 2 according to PCR6. X_A and $X_{B1} + X_{B2}$ are the masses added to the sets A and B respectively.

Consider the first example from Section III, given in Table 1. The redistribution can be illustrated by the diagram in Fig. 7, corresponding to the first partial conflict listed in Table 2.

As we can see, the mass that is moving to set B consists of two parts. The formulas are given below.

$$\begin{aligned} K &= m_1(A)m_2(B)m_3(B) \\ X_A &= \frac{m_1(A)}{m_1(A)+m_2(B)+m_3(B)}K \\ X_{B1} &= \frac{m_2(B)}{m_1(A)+m_2(B)+m_3(B)}K \\ X_{B1} &= \frac{m_3(B)}{m_1(A)+m_2(B)+m_3(B)}K \end{aligned} \quad (15)$$

Consider the diagram in Fig.8, for the second conflict in Table 2.

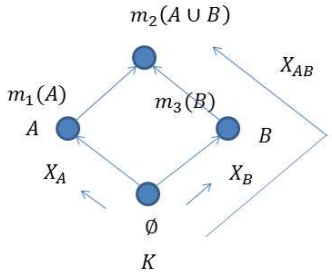

Figure 8 Redistribution of the second partial conflicting mass from Table 2 according to PCR6. X_A and X_B and X_{AB} are the masses added to the sets A, B, and AB respectively.

The difference between PCR5 and PCR6 is more prominent here since the set $A \cup B$ receives some mass in case of PCR6 and it did not receive any mass in the case of PCR5. The formulas are as follows.

$$\begin{aligned} K &= m_1(A)m_2(A \cup B)m_3(B) \\ X_A &= \frac{m_1(A)}{m_1(A)+m_2(A \cup B)+m_3(B)}K \\ X_{AB} &= \frac{m_2(A \cup B)}{m_1(A)+m_2(A \cup B)+m_3(B)}K \\ X_B &= \frac{m_3(B)}{m_1(A)+m_2(BA \cup B)+m_3(B)}K \end{aligned} \quad (16)$$

In light of these examples, the general procedure for PCR6 becomes clear.

Having presented PCR5 and PCR6 using the diagrams, we now seek a comparison of multiple sensors over multiple sets. The method supports both classification and tracking.

V. Performance Comparisons

In this section, we compare the performance of several fusion rules using simulated scenarios. The simulation is implemented for an arbitrary number of sensors S and possible targets N. We assume that each sensor can be assigned a confusion matrix that characterizes its classification accuracy.

If the true object is o_i and the sensor made a decision o_j, the corresponding confusion matrix entry is defined as $CM(i,j) = \Pr(o_j|o_i)$. This implies that, given that the sensor declared o_j, we get the probability mass assigned to the set of possible targets as $\Pr(o_i|o_j)$. This mass can be computed using Bayes formula, but we need to know the a priori target probabilities:

$$\Pr(o_i|o_j) = \frac{\Pr(o_j|o_i)\,\Pr(o_i)}{Z}. \qquad (17)$$

The denominator Z is the normalization factor. Thus, the rows of confusion matrix contain the probability distribution of the target declaration given the true target class. At each step of the simulation, we sample from the distribution given by $\Pr(\cdot\,|o_i)$. We then use the Bayes formula (17) to compute the posterior probabilities for each target. These probabilities are fused directly in the Bayesian fusion approach. In order to apply the belief function based approaches, we select the argument with the maximum posterior probability as the most likely target and assign the maximum posterior probability as the probability mass for this target. The rest of the probability mass is assigned to the sure event Ω. The bodies of evidence corresponding to each sensor are then combined with each other and with the body of evidence from the previous time step. The simulation procedure is outlined below. The generic $FUSE$ function in step 8 is substituted by a particular rule, such as PCR6, etc. Line 9 computes *pignistic* probabilities used for decision making, as described in [25].

Multi-sensor fusion simulation	
Given:	
N – number of targets	
S – number of sensors	
K_{max} – number of time steps in the simulation	
CM_s – confusion matrices, $s = 1..S$	
T_k-target type for time step k, $k = 1..K_{max}$	
$m_0(\Omega) = 1$, the initial bodies of evidence is total ignorance	
1.	For each time step k
2.	For each sensor s
3.	o_{sk} is a sample from $\Pr(o_{sk}\|T_k, s) \equiv CM_s(\cdot, T_k)$
4.	Compute $\Pr(o_{tk}\|o_{sk})$ for $o_{tk} = 1..N$
5.	$\bar{o}_{tk} = \arg\max_{o_{tk}} \Pr(o_{tk}\|o_{sk})$ – max a posteriori target
6.	Create body of evidence Ω_{sk}, such that
7.	$m_{sk}(\bar{o}_t) = \max_{o_t} \Pr(o_{tk}\|o_{sk})$ $m_{sk}(\Omega) = 1 - \max_{o_t} \Pr(o_{tk}\|o_{sk})$
8.	Combine previous fused body of evidence with the new bodies of evidence, $m_k = FUSE(m_{k-1}, m_{1k}, .., m_{Sk})$
9.	Compute pignistic probabilities from m_k, Bet_k
10.	Make target declaration based on the maximum Bet_k

A. Case 1: Tracking and Classification: 2 sources

A sample result of simulation is shown in Fig. 9. The true class of the observed target changes over time and thus conflict is introduced between the subsequent measurements. In addition, false target declarations cause conflict as well. The ability of different fusion methods to recover from these conflicts in a timely manner can be observed.

We set the number of time steps to 120, and perform 50 independent runs. The average values over 50 runs are shown in the Fig. 9, which is made for target class 1.

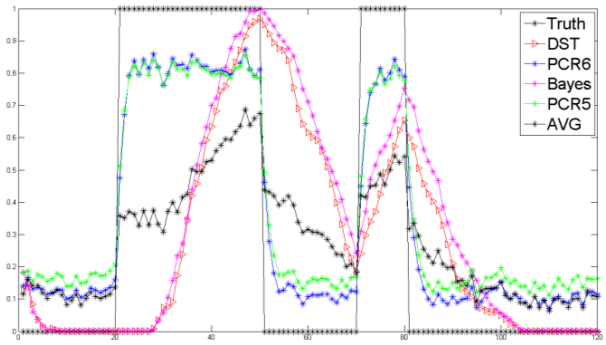

Figure 9 Target tracking and classification simulation, in case of *N*=2 possible targets and *S*=2 sources.

The "Truth" value equals to 0 when the true target class is not 1 and it equals to 1 when the true target class is 1. The plot shows how the probability mass assigned to target class 1 by the fused body of evidence changes over time, for 5 combination rules. As we can see, the PCR5 and PCR6 rules are the best at handling conflicting information which is reflected in the short transition time when the true target class switches (steps 20, 50, 70, and 80).

The classification accuracy of the fusion rules is estimated by dividing the number of steps with correct target class declaration by the total number of time steps. As it can be expected from Fig. 9, the accuracy of PCR5 and PCR6 is higher than the accuracy of DST and the other rules.

B. Tracking and Classification: S sources

In the next experiments, we ran the simulations with increasing number of sources. The results obtained for the 2 class case are shown in Fig. 10.

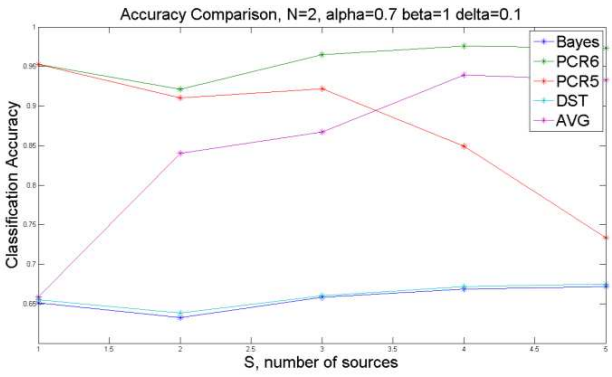

Figure 10 Classification accuracy of target tracking and classification in simulated scenarios with *S*=1,2,3,4, and 5 sources. AVG simply averages the bpa's.

These results show an interesting trend. As the number of sources increases, the performance of PCR5 significantly deteriorates. The other rules show consistent performance, with PCR6 resulting in the highest accuracy.

In our analysis, we used a variety of confusion matrices to represent the source classification used for the simulations; Table 5 shows some examples of randomly generated confusion matrices.

TABLE 5

CM1		CM2		CM3	
0.8992	0.1008	0.8763	0.1237	0.7364	0.2636
0.0647	0.9353	0.0717	0.9283	0.1908	0.8092
CM4		CM5			
0.6271	0.3729	0.6856	0.3144		
0.3071	0.6929	0.2756	0.7244		

In Fig. 11, we show another results of a similar experiment, where the number of time steps was set to 30 and the number of sources varied from 1 to 7. The cross-over point between PCR5 and PCR6 is between 3 and 4 sources. Again, the performance of PCR5 decreases to basically chance level for 6 and 7 sources (and less than DST).

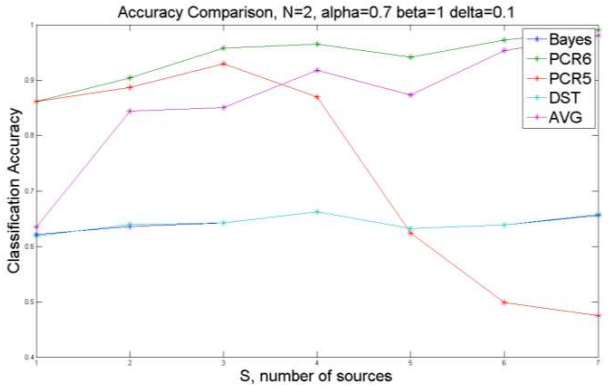

Figure 11 Classification accuracy of target tracking and classification in simulated scenarios with *S*=1 through 7 sources, for 2 targets. AVG simply averages the bpa's.

Note that in our simulation, the number of masses of evidence that need to be combined equals to the number of sources plus one as we combine the current time step evidence with the fused body of evidence from the next step. This explains why the performance of PCR5 and PCR6 is exactly the same for one source, since the procedures become identical when combining two bodies of evidence [6].

VI. DISCUSSION

In order to demonstrate the results presented in this work we have accomplished the following tasks.

1. Investigated PCR5 and PCR6 rules and presented them in graphical form. Although this is not a novel contribution, we believe that it significantly improves the readability of PCR rules by non-experts in the area.
2. Implemented PCR5 and PCR6 for *S* sources and *N* targets. Our implementation of PCR6 was compared against Arnaud Martin's toolbox implementation to yield identical numeric results. However, our implementation is significantly faster than Martin's. We were unable to find alternative PCR5 implementation to compare to our own.
3. Verified that PCR5 and PCR6 give the same results for *S*=2 and any number of targets *N*. This agreement with the theory boosted our confidence in our PCR5 implementation.
4. Implemented a simulation of multiple source target tracking and classification for arbitrary number of sources and possible targets.
5. Compared classification accuracy of PCR5, PCR6, DST, Average, and Bayes fusion rules for *N*=2 target tracking and classification problem for the number of sources *S*=1 through 7.

While there has not been a study of this kind reported, we found that PCR5 is not well suited for many sources. An obvious concern is that the implementation needs to be validated; however, as per the literature, the trend is consistent where PCR5 is not suggested for many sources. What is thus a contribution is that PCR5 is typically used with 2 sources of which we have shown that it is also useful for three sources. Its performance for more than three sources is lower than PCR6. We suggest that further independent investigations be conducted to compare PCR5 and PCR6. We also note that the average fusion rule demonstrated performance comparable to PCR6. This concurs with the recent work comparing PCR6 and average fusion rule [21].

VII. CONCLUSIONS

In this study, we have compared several fusion methods and demonstrated the improved performance of PCR5 and PCR6 over the classical Dempster-Shafer and Bayesian methodologies. Additionally, we utilized Hasse diagrams to improve the understandability of the PCR methods. Through a comparative study, the advantage of PCR6 over PCR5 for more than three sources was presented. Future work includes updating the comparison with developments in PCR such as the fuzzy-combination rules, combination of our implementation with latest techniques in tracking and situation modeling [26] [27], and utilization of our implementations with real data.

ACKNOWLEDGMENT

Support for this research was provided by the Air Force Office of Scientific Research, Department of the Air Force, grant number 14RY04COR as well as 13RI02COR from the DDDAS program. We utilized the Matlab toolbox from Arnaud Martin for DST computations and PCR6 verification, which was appreciated. Initial PCR5 developments were from Jean Dezert.

REFERENCES

[1] E. Blasch, J. Dezert and B. Pannetier, "Overview of Dempster-Shafer and Belief Function Tracking Methods," in *Signal Processing, Sensor Fusion, and Target Recognition XXII, Proc. of SPIE*, 2013.

[2] L. Hongfei, J. Hongbin, T. Kangsheng and F. Xiaoyan, "Analysis and Improvement for Proportional Conflict Redistribution Rules," in *International Conference on Computer Application and System Modeling*, 2010.

[3] F. Smarandache and J. Dezert, "Extended PCR Rules for Dynamic Frames," in *International Conference on Information Fusion*, 2012.

[4] F. Smarandache and J. Dezert, "Information Fusion Based on New Proportional Conflict Redistribution Rules," in *International Conf. on Information Fusion*, 2005.

[5] F. Smarandache and J. Dezert, "An Introduction to the DSm Theory for the Combination of Paradoxical, Uncertain, and Imprecise Sources of Information," 2006. [Online]. Available: http://www.gallup.unm.edu/~smarandache/DSmT.htm .

[6] A. Martin and C. Osswald, "A new generalization of the proportional conflict redistribution rule stable in terms of decision," in *Advances and Applications of DSmT for Information Fusion: Collected Works, Vol. II*, American Research Press, 2006.

[7] A. Martin, J. Dezert and F. Smarandache, "General combination rules for qualitative and quantitative beliefs," *J. of Adv. in Information Fusion,* vol. 3, no. 2, 2008.

[8] J. Dezert and F. Smarandache, Advances and applications of DSmT for information fusion (Collected works)], American Research Press, 2004-2009.

[9] E. Blasch, J. Dezert and P. Valin, "DSMT Applied to Seismic and Acoustic Sensor Fusion," in *Proc. IEEE Nat. Aerospace Electronics Conf (NAECON)*, 2011.

[10] E. Blasch, A. Jøsang, J. Dezert, P. C. G. Costa, K. B. Laskey and A.-L. Jousselme, "URREF Self-Confidence in Information Fusion Trust," in *Int'l. Conf. on Information Fusion*, 2014.

[11] H. Leung, Y. L. E. Bossé, M. Blanchette and K. C. C. Chan, "Improved multiple target tracking using Dempster-Shafer Identification," in *Proc. SPIE, Vol. 3068*, 1997.

[12] E. Blasch and L. Hong, "Simultaneous Tracking and Identification," in *IEEE Conference on Decision Control*, 1998.

[13] E. Blasch, *Derivation of a Belief Filter for Simultaneous High Range Resolution Radar Tracking and Identification, Ph.D. Thesis,* Wright State University, 1999.

[14] J. Dezert, . Tchamova, F. Smarandache and P. Konstantinova, "Target Type Tracking with PCR5 and Dempster's Rules: A Comparative Analysis," in *Int. Conf. on Information Fusion*, 2006.

[15] F. Dambreville, F. Celeste, J. Dezert and F. Smarandache, "Probabilistic PCR6 fusion rule, Ch 4," in *Advances and Applications of DSmT for Information Fusion: Collected Works, Vol. 3*, American Research Press, 2009.

[16] B. Pannetier and J. Dezert, "GMTI and IMINT data fusion for multiple target tracking and classification," in *Int. Conf. on Information Fusion*, 2009.

[17] J. Dezert and B. Pannetier, "A PCR BIMM filter for maneuvering target tracking," in *International Conference on Information Fusion*, 2010.

[18] Y. Sun and L. Bentabet, "A particle filtering and DSmT Based Approach for Conflict Resolving in case of Target Tracking with multiple cues," *Journal of Mathematical Imaging and Vision,* vol. 36, no. 2, pp. 159-167, 2010.

[19] A. Tchamova and J. Dezert, "Performance evaluation of fuzzy-based fusion rules for tracking applications," *International Journal of Reasoning-based Intelligent Systems,* pp. 1-9, 2014.

[20] J. Dezert and A. Tchamova, "On the Validity of Dempster's Fusion Rule and its Interpretation as a Generalization of Bayesian Fusion Rule," *International Journal of Intelligent Systems,* vol. 29, p. 223–252, 2014.

[21] F. Smarandache and J. Dezert, "On the Consistency of the PCR6 with the Averaging Rule and its Application to Probability Estimation," in *International Conference on Information Fusion*, 2013.

[22] D. Han, J. Dezert and Y. Yang, "Evaluations of Evidence Combination Rules in Terms of Statistical Sensitivity and Divergence," in *International Conf. on Information Fusion*, 2014.

[23] P. Smets, "The combination of evidence in the transferable belief model," in *Pattern Analysis and Machine Intelligence, IEEE Transactions on* , 1990.

[24] B. Davey and H. Priestley, Introduction to Lattices and Order, Cambridge: University Press, 2002.

[25] P. Smets, "Decision Making in the TBM: the necessity of the pignistic transformation," *International Journal of Approximate Reasoning,* vol. 38, pp. 133-147, 2005.

[26] R. Ilin and R. Deming, "Simultaneous detection and tracking of multiple objects in noisy and cluttered environment using maximum likelihood estimation framework," in *OCEANS 2010 IEEE*, Sydney, 2010.

[27] R. Ilin, "Unsupervised learning of categorical data with competing models," *Neural Networks and Learning Systems, IEEE ,* vol. 23, no. 11, pp. 1726-1737, 2012.